Human Mean Age 84 Years Determined by Relativistic Matter Wave and Anti-ageing Guidance

Huaiyang Cui
Department of Physics, Beihang University, Beijing, 102206, China
Email: hycui@buaa.edu.cn
(Feb 1, 2023, submitted to viXra)

Abstract: It is found that relativistic matter wave provides a biological clock for human beings. At the first, two examples are given to show the validity of the relativistic matter wave. Next, the sunspot period, earth's atmosphere circulation and human biological clock are investigated, the clock formula is derived. As the results, the period of sunspot cycle is calculated to be 10.93 years, the human mean age is calculated to be 84 years.

Key words: relativistic matter wave, sunspot cycle, biological clock.

1. Introduction

This year is 100th anniversary of the initiative of de Broglie matter wave. In 1923, the Louis de Broglie considered blackbody radiation as a gas of light quanta [1], he tried to reconcile the concept of light quanta with the phenomena of interference and diffraction. In 1923 and 1924, the concept that matter behaves like a wave was proposed by Louis de Broglie [2]. Today it is called as the de Broglie matter wave.

An effort has made to generalize the de Broglie matter wave to planetary wave for a long time, but never succeeded; traditional quantum theory cannot properly deal with gravity problems [3][4][5]. In recent years, generalized relativistic matter wave has been proposed and applied to the solar system to explain quantum gravity effects, this approach provides a new method for quantum gravity. The relativistic matter wave [6] is given by

$$\psi = \exp(\frac{i\beta}{c^3}\int_0^x (u_1 dx_1 + u_2 dx_2 + u_3 dx_3 + u_4 dx_4)) \quad . \tag{1}$$

where u is 4-velocity of particle, β is a constant determined by experiments. In this paper, at the first, two examples are given to show the validity of the relativistic matter wave; next, the sunspot period, earth's atmosphere circulation and human biological clock are investigated, the clock formula is derived. As the results, the period of sunspot cycle is calculated as 10.93 years, the human mean age is calculated as 84 years.

2. Example 1: determining the solar density and radius

As shown in Figure 1(a), the planetary circular orbit can be quantized in terms of the

relativistic matter wave as

$$\left.\begin{aligned}\frac{\beta}{c^3}\oint_L v_l dl = 2\pi n \\ v_l = \sqrt{\frac{GM}{r}}\end{aligned}\right\} \Rightarrow \sqrt{r} = \frac{c^3}{\beta\sqrt{GM}} n; \quad n = 0,1,2,\ldots \ . \tag{2}$$

This orbital quantization rule only achieves a partial success in the solar system, as shown in Figure 1(b), the Sun, Mercury, Venus, Earth and Mars satisfy the quantization equation; while other outer planets fail. In Figure 1(b), the blue straight line expresses a linear regression relation among the quantized orbits, so it gives β=2.961520e+10 (m/s^2). The quantum numbers n=3,4,5,... were assigned to the solar planets, the sun was assigned a quantum number n=0 because the sun is in the **central state**.

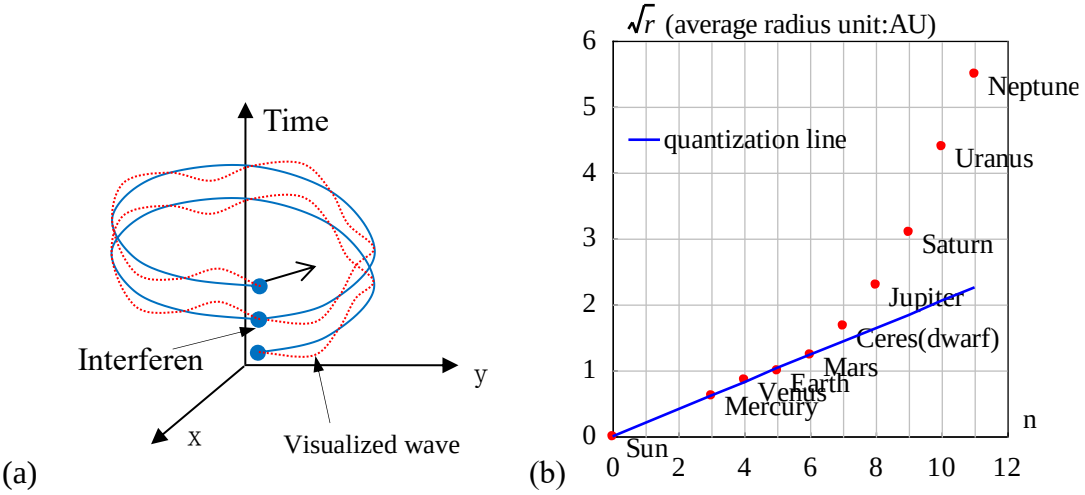

Figure 1 (a)The head of the relativistic matter wave may overlap with its tail. (b) The inner planets are quantized.

Since we only study quantum gravity effects among the Sun, Mercury, Venus, Earth and Mars, so this orbital quantization rule is good enough as a foundational quantum theory. For example, the relativistic matter wave can be applied to determine the solar density and radius.

In a central state n=0 with a size, if the coherent length of the relativistic matter wave is long enough, its head may overlap with its tail when the particle moves in a closed orbit in space-time, as shown in Figure 1(a). The overlapped wave is given by

$$\begin{aligned}\psi &= \psi(r)T(t) \\ \psi(r) &= 1 + e^{i\delta} + e^{i2\delta} + \ldots + e^{i(N-1)\delta} = \frac{1-\exp(iN\delta)}{1-\exp(i\delta)} \\ \delta(r) &= \frac{\beta}{c^3}\oint_L (v_l) dl = \frac{2\pi\beta\omega r^2}{c^3}\end{aligned} \ . \tag{3}$$

where N is the overlapping number which is determined by the coherent length of the relativistic matter wave, δ is the phase difference after one orbital motion, ω is the angular speed of the solar self-rotation. The above equation is a multi-slit interference formula in optics, for a larger N it is called as the Fabry-Perot interference formula.

The relativistic matter wave function ψ needs a further explanation. In quantum mechanics, $|\psi|^2$ equals to the probability of finding an electron due to Max Burn's explanation; in astrophysics, $|\psi|^2$ equals to the probability of finding a nucleon (proton or neutron) *averagely on an astronomic scale*, we have

$$|\psi|^2 \propto \text{nucleon-density} \propto \rho \quad . \tag{4}$$

It follows from the multi-slit interference formula that the overlapping number N is estimated by

$$N^2 = \frac{|\psi(0)_{multi-wavelet}|^2}{|\psi(0)_{one-wavelet}|^2} = \frac{\rho_{core}}{\rho_{surface\_gas}} \quad . \tag{5}$$

The solar core has a mean density of 1408 (kg/m^3), the surface of the sun is comprised of convective zone with a mean density of 2e-3 (kg/m^3) [7]. In this paper, the sun's radius is chosen at a location where density is 4e-3 (kg/m^3), thus the solar overlapping number N is calculated to be N=593.

Sun's angular speed at its equator is known as ω=2π/(25.05x24x3600) (s^{-1}). Its mass 1.9891e+30 (kg), well-known radius 6.95e+8 (m), mean density 1408 (kg/m^3), the constant β=2.961520e+10 (m/s^2). According to the N=593, the matter distribution of the $|\psi|^2$ is calculated in Figure 2, it agrees well with the general description of star's interior [8]. The radius of the sun is determined as r=7e+8 (m) with a relative error of 0.72% in Figure 2, which indicates that the sun radius strongly depends on the sun's self-rotation.

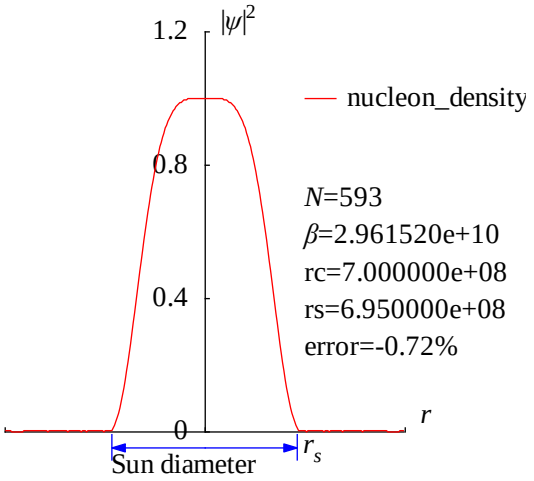

Figure 2 The nucleon distribution $|\psi|^2$ in the Sun is calculated in the radius direction.

```
<Clet2020 Script>//C source code
int i,j,k,m,n,N,nP[10];
double beta,H,B,M,r,r_unit,x,y,z,delta,D[1000],S[1000], a,b,rs,rc,omega,atm_height; char str[100];
main(){k=150;rs=6.95e8;rc=0;x=25.05;omega=2*PI/(x*24*3600);n=0; a=1408/0.004; N=sqrt(a);
beta=2.961520e10;H=SPEEDC*SPEEDC*SPEEDC/beta;M=1.9891E30; atm_height=2e6; r_unit=1E7;
for(i=-k;i<k;i+=1) {r=abs(i)*r_unit;
if(r<rs+atm_height) delta=2*PI*omega*r*r/H; else delta=2*PI*sqrt(GRAVITYC*M*r)/H;//around the star
x=1;y=0; for(j=1;j<N;j+=1) { z=delta*j; x+=cos(z);y+=sin(z);} z=x*x+y*y; z=z/(N*N);
S[n]=i;S[n+1]=z; if(i>0 && rc==0 && z<0.0001) rc=r; n+=2;}
SetAxis(X_AXIS,-k,0,k,"#ifr; ; ; ;");SetAxis(Y_AXIS,0,0,1.2,"#if|ψ|#su2#t;0;0.4;0.8;1.2;");
DrawFrame(FRAME_SCALE,1,0xafffaf); z=100*(rs-rc)/rs;
SetPen(1,0xff0000);Polyline(k+k,S,k/2,1," nucleon_density"); SetPen(1,0x0000ff);
r=rs/r_unit;y=-0.05;D[0]=-r;D[1]=y;D[2]=r;D[3]=y; Draw("ARROW,3,2,XY,10,100,10,10,",D);
Format(str,"#ifN#t=%d#n#ifβ#t=%e#nrc=%e#nrs=%e#nerror=%.2f%",N,beta,rc,rs,z);
TextHang(k/2,0.7,0,str);TextHang(r+5,y/2,0,"#ifr#sds#t");TextHang(-r,y+y,0,"Sun diameter");
}#v07=?>A
```

3. Example 2: determining the earth's density and radius

The moon is assigned a quantum number of n=2 because some quasi-satellite's perigees have reached a depth almost at n=1 orbit, as shown in Figure 3. Here, the constant β=1.377075e+14(m/s^2) is determined uniquely by the line between the earth and moon by Eq. (2).

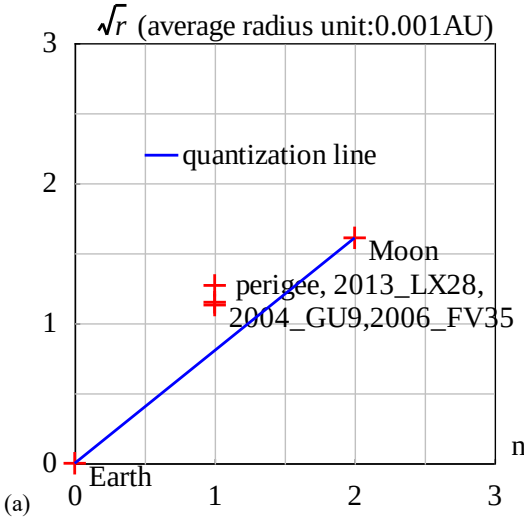

Figure 3 Orbital quantization for the moon.

The earth has a mean density of 5530 (kg/m^3), its surface is covered with air and vapor with a density of 1.29 (kg/m^3). The earth's radius is chosen at the sea level, it follows Eq.(5) that the earth's overlapping number N is calculated to be N=65.

The earth's angular speed is known as ω=2π/(24x3600) (s^{-1}), its mass 5.97237e+24 (kg), the well-known radius is 6.371e+6 (m), the earth constant β=1.377075e+14 (m/s^2). The matter distribution $|\psi|^2$ in radius direction is calculated by Eq.(3), as shown in Figure 4(a). The radius of the earth is determined as r=6.4328e+6 (m) with a relative error of 0.86%, it agrees well with common knowledge. The secondary peaks over the atmosphere up to 2000 km altitude are calculated in Figure 4(b) which agree well with the space debris observations [9][10][11].

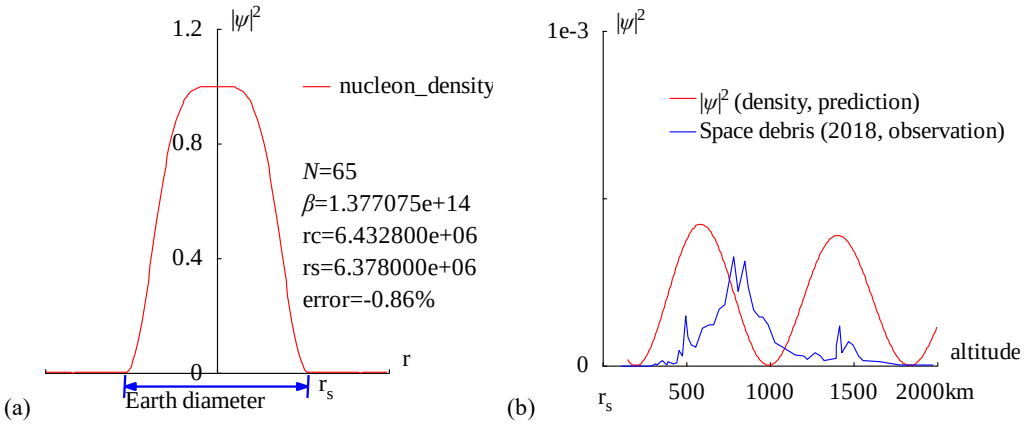

Figure 4 (a) The radius of the Earth is calculated out r=6.4328e+6 (m) with a relative error of 0.86% by the interference of its relativistic matter wave; (b) The prediction of the space debris distribution up to 2000 km altitude.

```
<Clet2020 Script>//C source code
int i,j,k,m,n,N,nP[10]; double H,B,M,v_r,r,AU,r_unit,x,y,z,delta,D[10],S[1000];
double rs,rc,rot,a,b,atm_height,beta; char str[100];
main(){k=80;rs=6.378e6;rc=0;atm_height=1.5e5;n=0; N=65;
beta=1.377075e+14;H=SPEEDC*SPEEDC*SPEEDC/beta;
M=5.97237e24;AU=1.496E11;r_unit=1e-6*AU; rot=2*PI/(24*60*60);//angular speed of the Earth
for(i=-k;i<k;i+=1) {r=abs(i)*r_unit;
if(r<rs+atm_height) v_r=rot*r*r; else v_r=sqrt(GRAVITYC*M*r);//around the Earth
delta=2*PI* v_r/H; y=SumJob("SLIT_ADD,@N,@delta",D); y=y/(N*N);
if(y>1) y=1; S[n]=i;S[n+1]=y; if(i>0 && rc==0 && y<0.001) rc=r;   n+=2;}
SetAxis(X_AXIS,-k,0,k,"r; ; ; ;");SetAxis(Y_AXIS,0,0,1.2,"#if|ψ|#su2#t;0;0.4;0.8;1.2;");
DrawFrame(FRAME_SCALE,1,0xafffaf); x=50;z=100*(rs-rc)/rs;
SetPen(1,0xff0000);Polyline(k+k,S,k/2,1," nucleon_density");
r=rs/r_unit;y=-0.05;D[0]=-r;D[1]=y;D[2]=r;D[3]=y;
SetPen(2,0x0000ff); Draw("ARROW,3,2,XY,10,100,10,10,",D);
Format(str,"#ifN#t=%d#n#ifβ#t=%e#nrc=%e#nrs=%e#nerror=%.2f%",N,beta,rc,rs,z);
TextHang(k/2,0.7,0,str);TextHang(r+5,y/2,0,"r#sds#t");TextHang(-r,y+y,0,"Earth diameter");
}#v07=?>A#t
```

```
<Clet2020 Script>//C source code
int i,j,k,m,n,N,nP[10]; double H,B,M,v_r,r,AU,r_unit,x,y,z,delta,D[10],S[10000];
double rs,rc,rot,a,b,atm_height,p,T,R1,R2,R3; char str[100]; int
Debris[96]={110,0,237,0,287,0,317,2,320,1,357,5,380,1,387,4,420,2,440,3,454,14,474,9,497,45,507,26,527,19,557,17,597,34,63
4,37,664,37,697,51,727,55,781,98,808,67,851,94,871,71,901,50,938,44,958,44,991,37,1028,21,1078,17,1148,10,1202,9,1225,6,
1268,12,1302,9,1325,5,1395,7,1395,18,1415,36,1429,12,1469,22,1499,19,1529,9,1559,5,1656,4,1779,1,1976,1,};
main(){k=80;rs=6.378e6;rc=0;atm_height=1.5e5;n=0; N=65;
H=1.956611e11;M=5.97237e24;AU=1.496E11;r_unit=1e4;
rot=2*PI/(24*60*60);//angular speed of the Earth
b=PI/(2*PI*rot*rs*rs/H); R1=rs/r_unit;R2=(rs+atm_height)/r_unit;R3=(rs+2e6)/r_unit;
for(i=R2;i<R3;i+=1) {r=abs(i)*r_unit; delta=2*PI*sqrt(GRAVITYC*M*r)/H;
y=SumJob("SLIT_ADD,@N,@delta",D); y=1e3*y/(N*N);// visualization scale:1000
if(y>1) y=1; S[n]=i;S[n+1]=y;n+=2;}
SetAxis(X_AXIS,R1,R1,R3,"altitude; r#sds#t;500;1000;1500;2000km ;");
SetAxis(Y_AXIS,0,0,1,"#if|ψ|#su2#t;0; ;1e-3;");DrawFrame(FRAME_SCALE,1,0xafffaf); x=R1+(R3-R1)/5;
SetPen(1,0xff0000);Polyline(n/2,S,x,0.8,"#if|ψ|#su2#t (density, prediction)");
for(i=0;i<48;i+=1) {S[i+i]=R1+(R3-R1)*Debris[i+i]/2000; S[i+i+1]=Debris[i+i+1]/300;}
SetPen(1,0x0000ff);Polyline(48,S,x,0.7,"Space debris (2018, observation) "); }#v07=?>A#t
```

4. Period of sunspot cycle

The **coherence length** of waves is usually mentioned but the **coherence width** of waves is rarely discussed in quantum mechanics, simply because the latter is not a matter for electrons, nucleon, or photons, but it is a matter in astrophysics. The analysis of observation data tells us that on the planetary scale, the coherence width of relativistic matter waves can extend to 1000 kilometers or more, as illustrated in Figure 5(a), the overlap may even occur in the width direction, thereby bringing new aspects to wave interference.

In the solar convective zone, adjacent convective arrays form a top-layer flow, a middle-layer gas, and a ground-layer flow, similar to the concept of **molecular current** in electromagnetism. Considering one convective ring at the equator as shown in Figure 5(b), there is an apparent velocity difference between the top-layer flow and the middle-layer gas, where their relativistic matter waves are denoted respectively by

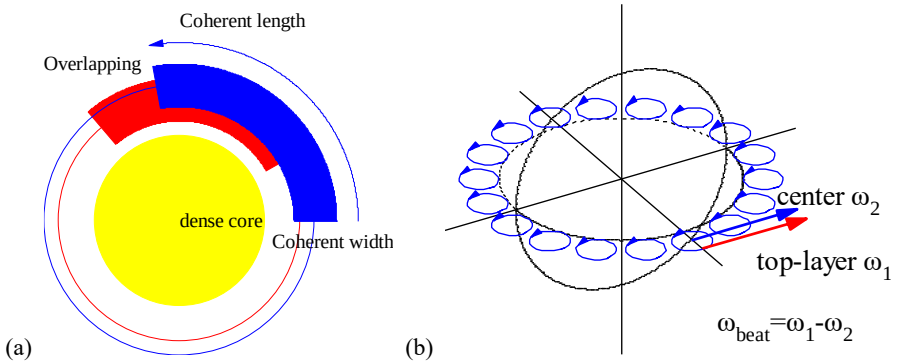

Figure 5 (a) Illustration of overlapping in the coherent width direction. (b) In convective rings at the equator, the speed difference causes a beat frequency.

$$\begin{aligned}
&\psi = \psi_{top} + C\psi_{middle} \\
&\psi_{top} = \exp[\frac{i\beta}{c^3}\int_L (v_1 dl + \frac{-c^2}{\sqrt{1-v_1^{\,2}/c^2}}dt)] \\
&\psi_{middle} = \exp[\frac{i\beta}{c^3}\int_L (v_2 dl + \frac{-c^2}{\sqrt{1-v_2^{\,2}/c^2}}dt)]
\end{aligned} \quad . \tag{6}$$

Their interference in the coherent width direction leads to a beat phenomenon

$$\begin{aligned}
&|\psi|^2 = |\psi_{top} + C\psi_{middle}|^2 = 1 + C^2 + 2C\cos[\frac{2\pi}{\lambda_{beat}}\int_L dl - \frac{2\pi}{T_{beat}}t] \\
&\frac{2\pi}{T_{beat}} = \frac{\beta}{c^3}(\frac{c^2}{\sqrt{1-v_1^{\,2}/c^2}} - \frac{c^2}{\sqrt{1-v_2^{\,2}/c^2}}) \simeq \frac{\beta}{c^3}(\frac{v_1^{\,2}}{2} - \frac{v_2^{\,2}}{2}) \\
&\frac{2\pi}{\lambda_{beat}} = \frac{\beta}{c^3}(v_1 - v_2); \quad V = \frac{\lambda_{beat}}{T_{beat}} = \frac{1}{2}(v_1 + v_2)
\end{aligned} \quad . \tag{7}$$

Their speeds are calculated as

$$\begin{aligned}
&v_1 \approx 6100\,(m/s) \quad (\approx \text{observed in Evershed flow}) \\
&v_2 = \omega r_{middle} = 2017\,(m/s) \quad (\text{solar rotation});
\end{aligned} \quad . \tag{8}$$

Where, regarding Evershed flow as the eruption of the top-layer flow, about 6 (km/s) speed was reported [12]. Alternatively, the top-layer speed v_1 also can be calculated in terms of thermodynamics, to be v_1=6244 (m/s) [6]. Here using v_1=6100 (m/s), their beat period T_{beat} is calculated to be a very remarkable value of 10.93 (years), in agreement with the sunspot cycle value (say, mean 11 years).

$$T_{beat} \simeq \frac{4\pi c^3}{\beta\left(v_1^{\,2} - v_2^{\,2}\right)} = 10.93\,(years) \quad . \tag{9}$$

The relative error to the mean 11 years is 0.6% for the beat period calculation using the relativistic matter waves. This beat phenomenon turns out to be a **nucleon density oscillation** that undergoes to drive the sunspot cycle evolution. The beat wavelength λ_{beat} is too long to observe, only the beat period is easy to be observed. As shown in Figure 6, on the solar surface, the equatorial circumference $2\pi r$ only occupies a little part of the beat wavelength, what we see is the expansion and contraction of the nucleon density.

$$\frac{2\pi r}{\lambda_{beat}} = 0.0031 \quad . \tag{10}$$

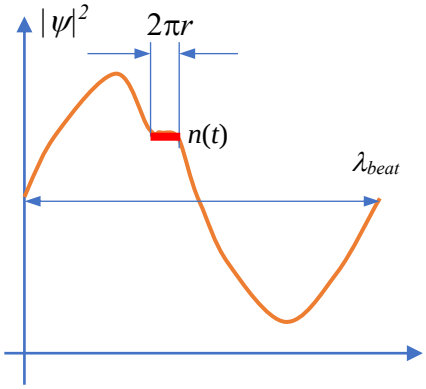

Figure 6 The equatorial circumference 2πr only occupies a little part of the beat wavelength, what we see is the expansion and contraction of the nucleon density.

This nucleon density oscillation is understood as a new type of nuclear reaction on an astronomic scale.

In the above calculation, although this seems to be a rough model, there is an obvious correlation between solar radius, solar rotation, solar density, and solar constant β.

5. Atmospheric circulation

Consider a relativistic matter wave ψ_A in the earth shell at the latitude angle A, it will interfere with its neighbor waves within its coherent width. Because the earth shell mainly consists of dense matter, their mutual cascade-interference will cause the relativistic matter waves to have spherical symmetry, so that the relativistic matter wave ψ_A at the latitude angle A should equal to the $\psi_{equator}$, as shown in Figure 7(a). This property is supported by the spherical symmetry of the earth's density distribution:

$$\text{spherical symmetry: } \rho(r,A,\varphi)=\rho(r) \quad \Rightarrow \quad \psi(r,A,\varphi)=\psi(r) \qquad (11)$$
$$\text{or: } \psi_A=\psi_{equator}$$

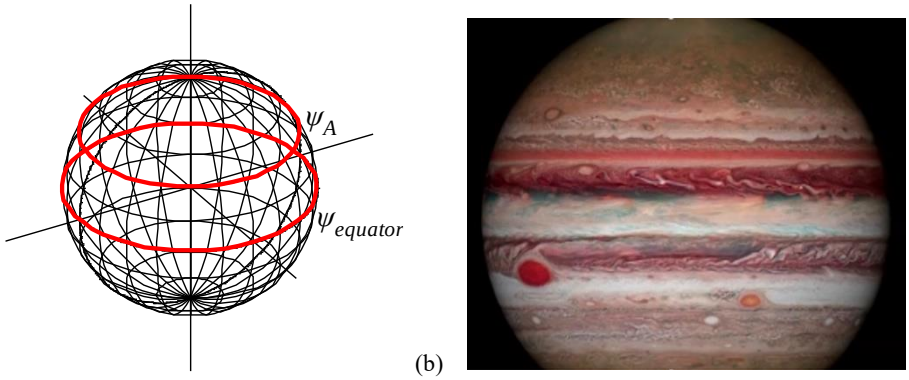

(a) (b)

Figure 7 (a) Mutual cascade-interference will lead to the symmetry of the earth's density distribution. (b) Zonal winds on Jupiter (the photo from public News).

On the contrary, in the thin atmosphere, the cascade-interference within coherence width can be ignored, so the wind and clouds are widely distributed in the sky on a large

scale.

Using the coherent width concept, considering the interference between the air ψ_A at the latitude angle A and the shell ψ_{shell} at the same latitude, their interference is

$$\begin{aligned}
&\psi(r,A)=\psi_{air}(r,A)+C\psi_{shell}(r,A)=\psi_{air}(r,A)+C\psi_{shell_equator}(r)\\
&T_{beat}\simeq\frac{4\pi c^3}{\beta\left(v_{shell_equator}{}^2-v_{air}{}^2\right)}\\
&v_{shell_equator}=\omega r\\
&v_{air}=\omega r\cos(A)+v_{wind}+v_{sun_effect}
\end{aligned}\quad . \tag{12}$$

where C represents the coupling constant which relates to their distance and mass fractions, their interference leads to a beat phenomenon. Positive wind represents the direction from west to east. The air is subjected to the solar radiation which enforces the beat oscillation to run at the period T_{beat}=1 (year) at the latitude angles A=23.5°S ~ 23.5°N due to the tilt of the earth axis with respect to the earth's orbital plane.

Suppose in spring the sun directly shines on latitude A_1=12°N on the northern hemisphere, where the atmosphere undergoes a beat T_{beat}=1 (year) with zero wind due to the constructive interference with the sun. This mostly shined latitude A_1 is called as the first constructive interference ridge, with zero wind, using the above beat period formula we obtain the sun effect:

$$v_{sun\_effect}=369.788-\omega r\cos(A_1);\quad (units: m/s)\ . \tag{13}$$

At the same time, the sun effect at other latitude A should be

$$v_{sun\_effect}=369.788\cos(A-A_1)-\omega r\cos(A)\ . \tag{14}$$

Thus, it follows the beat period formula that the wind under control of the beat T_{beat} is given by

$$v_{wind}=\sqrt{\omega^2r^2-\frac{4\pi c^3}{\beta T_{beat}}}-\omega r\cos(A)-v_{sun\_effect}\ . \tag{15}$$

It is not easy to maintain the constructive interference condition for these waves. When the first constructive interference ridge is at latitude A_1=12°N, the wind required for maintaining the beat T_{beat}=1 (year) near the latitude A=12°N is calculated by Eq.(15) as shown in Figure 8(a) (blue line), this wind will be destroyed by destructive interference at higher latitudes. But, the wind will arise up again at the next locations where the waves again satisfy the constructive interference condition: at A=39°N location (second ridge) where beat T_{beat}=0.5 (years), and at A=57°N location (third ridge) where beat T_{beat}=0.37 (years) which is the shortest period that the earth can get within the arctic regions. The maximal wind appears most probably at the midpoint of the first two ridges, about 48 (m/s). Linking all characteristic points in Figure 8(a) we obtain the predicted wind-curve over the northern hemisphere; this prediction agrees well with the experimental observations at an altitude of 10km (200hPa), as shown in Figure 9.

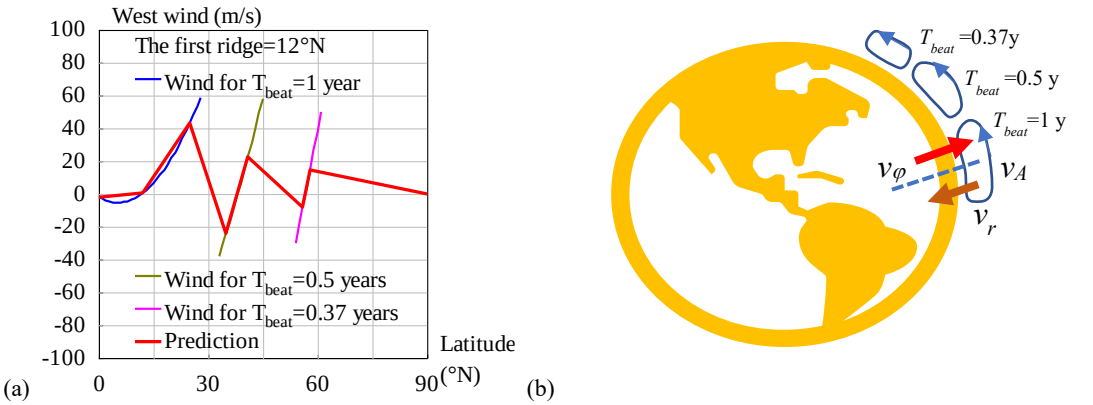

Figure 8 (a) Calculation of west winds in the northern hemisphere. (b) The atmospheric circulation in the northern hemisphere.

```
<Clet2020 Script>//C source code
double beta,H,M,r,rc, rs, rot,v1,v2, Year,T,Lamda,V,a,b,w,Fmax,N[500],S[500],F[100]; int i, j, k, t, m, n, s, f,Type,x;
int main(){beta=1.377075e+14; H=SPEEDC*SPEEDC*SPEEDC/beta;
M=5.97237e24; rs=6.371e6; rot=2*PI/(24*3600); Year=24*3600*365.2422;
Type=1; x=10; if(Type>1) x=-30;//v2=rs*rot; a=v2*v2-4*PI*H/Year; V=sqrt(a)-v2;
if(Type==1)   SetAxis(X_AXIS,0,0,90,"Latitude#n(°N);0;30;60;90;");
else   SetAxis(X_AXIS,-90,-90,90,"Latitude#n(°N);=90;-60;-30;0;30;60;90;");
SetAxis(Y_AXIS,-100,-100,100,"West wind (m/s);-100;-80;-60;-40;-20;0;20;40;60;80;100;");
DrawFrame(0x016a,Type,0xafffaf);//Polyline(2,"-90,0,90,0");
Check(15,k); if(k>24) k=24; if(k<-24) k=-24; //TextAt(100,10,"V=%f",V);
T=Year/2; Wind(); f=0; Findf(); t=N[m+m]; T=Year; Wind(); f=0; Findf();
SetPen(2,0xff); Polyline(n,N,x,70,"Wind for T#sdbeat#t=1 year"); if(Type>1) Polyline(s,S);
F[0]=N[0];F[1]=N[1]; F[2]=N[m+m]; F[3]=N[m+m+1];   t=(t+F[2])/2;//midst of two ridges
  t=t-F[2]+m; Fmax=N[t+t+1]; //TextAt(100,20,"t=%d, Fmax=%f ",t,Fmax);
f=Fmax; Findf(); F[4]=N[m+m]; F[5]=N[m+m+1];
T=Year/2; Wind(); f=-Fmax/2; Findf(); t=m;f=Fmax/2; Findf();
SetPen(2,0x80ff00); Polyline(n,N,x,-50,"Wind for T#sdbeat#t=0.5 years"); if(Type>1) Polyline(s,S);
F[6]=N[t+t]; F[7]=N[t+t+1];   F[8]=N[m+m]; F[9]=N[m+m+1];
T=0.37*Year; Wind(); f=-Fmax/4; Findf(); t=m;f=Fmax/4; Findf();
SetPen(2,0x9933fa); Polyline(n,N,x,-70,"Wind for T#sdbeat#t=0.37 years"); if(Type>1) Polyline(s,S);
F[10]=N[t+t]; F[11]=N[t+t+1];   F[12]=N[m+m]; F[13]=N[m+m+1];   F[14]=90; F[15]=0;
//Draw("ELLIPSE,0,2,XYX,10","15,20,25,35");TextHang(5,40,0,"a route");
SetPen(3,0xff0000); Polyline(8,F,x,-90,"Prediction"); TextHang(x,90,0,"The first ridge=%d°N", k);
}
Wind(){n=0;s=0;
for(i=0;i<90;i+=1)   { a=i*PI/180; b=(i-k)*PI/180; v1=rot*rs*cos(a); v2=rot*rs;
w=369.788*cos(b)-v2*cos(k*PI/180); a=v2*v2-4*PI*H/T; V=sqrt(a)-v1-w;
if(V>-40 && V<60) {N[n+n]=i; N[n+n+1]=V; n+=1;}}
for(i=0;i<90;i+=1)   { a=-i*PI/180; b=(-i-k)*PI/180; v1=rot*rs*cos(a); v2=rot*rs;
w=369.788*cos(b)-v2*cos(k*PI/180); a=v2*v2-4*PI*H/T; V=sqrt(a)-v1-w;
if(V>-40 && V<60) {S[s+s]=-i; S[s+s+1]=V; s+=1;}} }
Findf(){a=1e10; for(i=0;i<n;i+=1)   { b=N[i+i+1]-f ;if(b<0) b=-b;if(b<a) {m=i;a=b;}}
}//if(k==12) ClipJob(APPEND,"i=%d,V=%f",i,V);
#v07=?>A
```

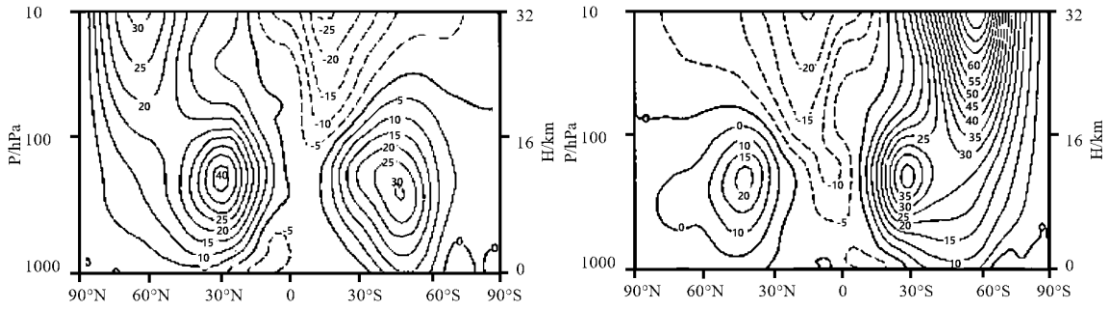

Figure 9 NCEP/NCAR data, mean west winds over 40 years (1958~1997) [13]. (a) winter; (b) summer.

For further improvement of precision, the value of the wind required by the constructive interference condition should be understood as a magnitude, it should be resolved into three components in the spherical coordinates (r, A, φ) as

$$v_{wind}^{\ 2} = v_r^{\ 2} + v_A^{\ 2} + v_\varphi^{\ 2} \ . \tag{16}$$

According to the energy equipartition theorem in thermodynamics, approximately we have the average estimation

$$< v_r^{\ 2} >=< v_A^{\ 2} >=< v_\varphi^{\ 2} >= \frac{1}{3} v_{wind}^{\ 2} \ . \tag{17}$$

Thus, the wind vectors around the northern hemisphere of the Earth are plotted in Figure 8(b), where the atmospheric circulation consists of three cells: Hadley cell, Ferrel cell, and arctic cell.

The beat T_{beat}=1 (years) works out **two seasons** in the equatorial regions. The beat T_{beat}=0.5 (years) blows comfortable winds over Europe, Northern America and Northeastern Asia, and modulates out **four seasons**; the shortest beat T_{beat}=0.37 (years) has a beat wavelength too long to be confined in the arctic regions so that it escapes from the north pole toward the equator, so recognized as the planetary scale waves or **Rossby waves**; in other words, the arctic regions can contain T_{beat}=1/3 (years) while emitting extra cold streams per 2.24 years to Europe, Northern America and Northeastern Asia. The zonal winds on the Jupiter has the same characteristics, as shown in Figure 7(b).

Since the relativistic matter wave of the air interferes with the relativistic matter wave of the earth shell, the easterlies at the equator have a magnitude of about 10 m/s in Figure 8(a). The trade winds or easterlies are the permanent east-to-west prevailing winds that flow in the Earth's equatorial region.

6. Human biological clock

Human body consists of five parts: one head and four limbs, a heart pumps the blood to the whole body circularly. Consider a person sleeping in a bed with the head pointing to the North Pole, as shown in Figure 10(a), the five red lines from the heart represent its five artery tubes.

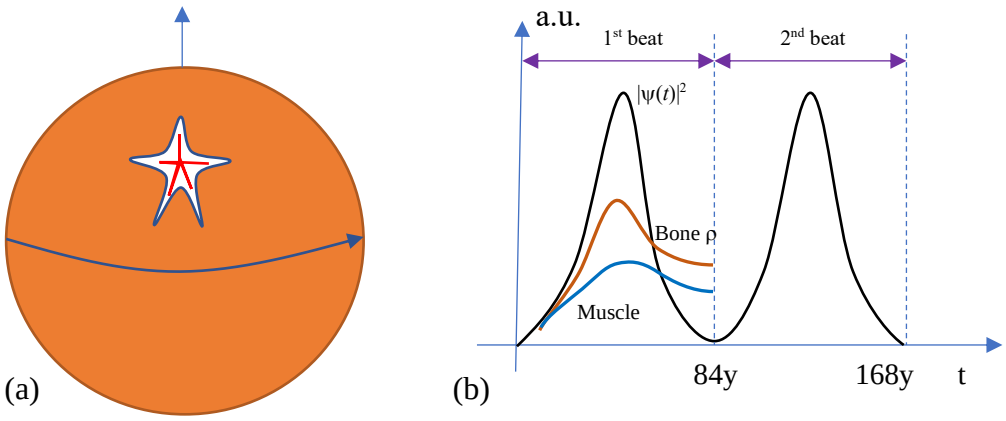

Fig.10 (a)A human sketch with the head pointing to the North Pole. (b) the biological clock.

Apparently, the arterial blood flows into the two arms with a speed whose matter wave would interfere with the Earth's rotation. The relativistic matter wave of the

flowing blood interferes with that of the Earth's shell, producing a beat phenomenon:

$$|\psi|^2=|\psi_{blood}+C\psi_{shell}|^2=1+C^2+2C\cos[\frac{2\pi}{\lambda_{beat}}\int_L dl-\frac{2\pi}{T_{beat}}t]$$
$$\frac{2\pi}{T_{beat}}=\simeq\frac{\beta}{c^3}(\frac{v_{blood}{}^2}{2}-\frac{v_{shell}{}^2}{2});\quad \frac{2\pi}{\lambda_{beat}}=\frac{\beta}{c^3}(v_{blood}-v_{shell});\quad v_{shell}=\omega r \qquad (18)$$

where C represents the coupling constant, ω is the Earth's angular speed, r the Earth radius. The blood flow velocity varies with the location of blood vessels. The normal value of aortic valve orifice blood flow velocity in adults is 1.0-1.7m/s, and that in children is 1.2-1.8cm/s. The flow velocity of carotid artery is less than 1.2 m/s, the normal flow velocity of abdominal aorta is less than 1.8 m/s, and the normal flow velocity of inferior vena cava is 5-25 cm/s. So, 1m/s is the order of magnitude of the blood velocity. Suppose the mean blood speed in human arms is 1m/s near the heart, then the flowing blood suffers a beat with the period as the follows

$$v_{shell}=r\omega=463.8m/s;\quad v_{blood}=v_{shell}\pm 1m/s$$
$$T_{beat}\simeq\frac{4\pi c^3}{\beta\left(v_{blood}{}^2-v_{shell}{}^2\right)}=\pm 84\,(years);\quad \lambda_{beat}=1.2e+12(m) \qquad (19)$$

```
<Clet2020 Script>// [14]
double beta,H,M,r,rc, rs, rot,v1,v2, Year,T,Lamda,V,a,b,x,y,w;
int main(){beta=1.377075e+14; H=SPEEDC*SPEEDC*SPEEDC/beta;
M=5.97237e24; rs=6.378e6; rot=2*PI/(24*3600); Year=24*3600*365.2422;
v1=rot*rs;v2=v1+1; a=v2*v2-v1*v1; T=4*PI*H/a;
T/=Year; Lamda=2*PI*H/(v2-v1); b=Lamda/(2*PI*rs);
TextAt(100,20,"v1=%f, v2=%f, T=%f, L=%e, b=%e",v1,v2,T,Lamda,b);
}#v07=?>A
```

In the fact, the blood is pumped from the heart into both the eastern arm and western arm in Figure 10(a), producing a positive beat and a negative beat in the two arms with the same period 84 years, the two beats form an overall beat through the two arms. It is found that human mean lifetime is just confined within the single period duration, recognized as the **human biological clock**. The beat wavelength λ is 30000 times the circumference of the earth, so its λ effects are hardly observed.

According to the explanation to ψ in the preceding section, the beat $|\psi|^2$ represents the probability of finding a nucleon on a macro-scale, in other words, the $|\psi|^2$ is proportional to the matter density.

$$|\psi|^2\propto\rho \qquad (20)$$

The $|\psi|^2$ oscillation of the beat in Figure 10(b) represents the variation of a human body density in his whole life confined within one beat period. The human bone density (red line) and muscle (blue line) in a human life vary as function of age, also responding to the $|\psi|^2$ oscillation, as shown in Figure 10(b).

Obviously, the human bone and muscle are irreversible for the life process, they also completely resist the human to enter into the second beat for obtaining a 168 years longevity. Perhaps, some soft animals or cells may enter multi-beat process for a longer life or immortal. Sleep position, walking, running, sitting down, etc. may make influences on the human biological clock in some extent, cannot stop ticking of the human biological clock, because the blood never stops as the life.

7. Guidance of anti-ageing

In the preceding section, we have derived the formula of human lifetime, consequently, increasing mean blood speed near human heart will lead to life reduction; decreasing mean blood speed near human heart will lead to life extension. For pursuing life extension or anti-ageing, some ideas are devised as follows.

(1) Sleeping position

At the first, the head must point to the North Pole so that the projection component of the blood velocities in various parts of the body in the direction of the earth's rotation has a relatively small value which favor the life extension. Next, lying on a side also reduces the projection component of the blood velocities in the direction of the earth's rotation, comparing to the lying-stretched out, as illustrated in Figure 11(a).

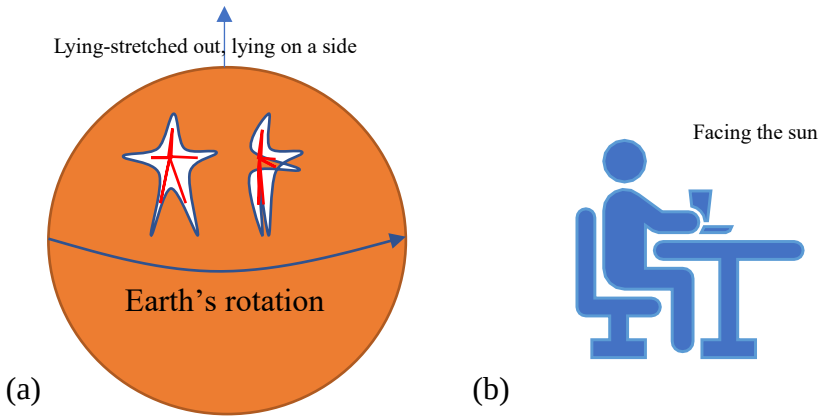

Fig.11 Lying-stretched out, lying on a side with the head pointing to the North Pole.

(2) Medicines

No doubt, some medicines can adjust the blood velocities in various parts of the human body. Normally, drinking tea, coffee, alcohol, etc. can increase the speed of blood in the human body for a while, leading to an accumulated effect for reducing the lifetime. Hydrophilic compounds such as alum can decease blood velocities in various parts of the body, but they are also appearing side and toxical effects for life bodies.

As we known, some Chinese traditional herbs can decease human blood velocities with less toxical effects, actually ancient Chinese didn't know how the herbs to work, today we understood.

(3) Office time

In china, office workers such as programmers, clerks, teachers, etc. spend 8 hours a day in offices. For weakening the coupling effects between blood velocities in human body and the earth's rotation for human life extension, workers need face the sun (east or west) when sitting for several hours, as illustrated in Figure 11(b). It is also suggested for the workers to drink cold-water or cold foods.

(4) Architecture and environment

Almost all people spend their lives in rooms or buildings, architecture and environment have great impact on human lifetime. Many efforts in accordance with the quantum gravity theory [15][16][17] are required to be made so that these architectures benefit human activities.

8. Conclusions

It is found that relativistic matter wave provides a biological clock for human beings. At the first, two examples are given to show the validity of the relativistic matter wave. Next, the sunspot period, earth's atmosphere circulation and human biological clock are investigated, the clock formula is derived. As the results, the period of sunspot cycle is calculated to be 10.93 years, the human mean age is calculated to be 84 years.

References

[1] de Broglie, L. (1923) Waves and Quanta. Nature, 112, 540. https://doi.org/10.1038/112540a0

[2] de Broglie, L. (1925) Recherches sur la théorie des Quanta, Translated in 2004 by A. F. Kracklauer as De Broglie, Louis, on the Theory of Quanta. https://doi.org/10.1051/anphys/192510030022

[3] Marletto, C. and Vedral, V. (2017) Gravitationally Induced Entanglement between Two Massive Particles Is Sufficient Evidence of Quantum Effects in Gravity. Physical Review Letters, 119, Article ID: 240402. https://doi.org/10.1103/PhysRevLett.119.240402

[4] Guerreiro, T. (2020) Quantum Effects in Gravity Waves. Classical and Quantum Gravity, 37, Article ID: 155001. https://doi.org/10.1088/1361-6382/ab9d5d

[5] Carlip, S., Chiou, D., Ni, W. and Woodard, R. (2015) Quantum Gravity: A Brief History of Ideas and Some Prospects, International Journal of Modern Physics D, 24, Article ID: 1530028. https://doi.org/10.1142/S0218271815300281

[6] Cui, H.Y. (2021) Relativistic Matter Wave and Quantum Computer. Kindle Ebook.

[7] NASA. https://solarscience.msfc.nasa.gov/interior.shtml

[8] Schneider, S.E. and Arny, T.T. (2018) Pathways to Astronomy. 5th Edition, McGraw-Hill Education, London.

[9] Orbital Debris Program Office, (2018) History of On-Orbit Satellite Fragmentations. 15th Edition, National Aeronautics and Space Administration, Washington DC.

[10] Wright, D. (2007) Space Debris. Physics Today, 10, 35-40. https://doi.org/10.1063/1.2800252

[11] Tang, Z.-M., Ding, Z.-H., Dai, L.-D., Wu, J. and Xu, Z.-W. (2017) The Statistics Analysis of Space Debris in Beam Parking Model in 78˚ North Latitude Regions. Space Debris Research, 17, 1-7.

[12] Cox, N. (2001) Allen's Astrophysical Quantities. 4th Edition, Springer-Verlag, Berlin. https://doi.org/10.1007/978-1-4612-1186-0

[13] Li,L.P. et al, (2021) Introduction to Atmospheric Circulation, 2nd edition, Science Press.

[14] Clet Lab (2022) Clet: C Compiler. https://drive.google.com/file/d/1OjKqANcgZ-9V56rgcoMtOu9w4rP49sgN/view?usp=sharing

[15] Cui,H.Y. (2022) Study of Earthquakes in Japanese Islands Using Quantum Gravity Theory with Ultimate Acceleration, viXra:2209.0149, 2022. https://vixra.org/abs/2209.0149

[16] Cui,H.Y. (2022) Study of European Cold Streams Per 2.24 Years Based on Quantum Gravity Theory with Ultimate Acceleration,viXra:2211.0051,2022. https://vixra.org/abs/2211.0051

[17] Cui,H.Y. (2023) Determination of Solar Radius and Earth's Radius by Relativistic Matter Wave, Journal of Applied Mathematics and Physics, 11, 1, DOI: 10.4236/jamp.2023.111006